Initial-value predictability of Antarctic sea ice in the Community Climate System Model 3

Marika M. Holland,[1] Edward Blanchard-Wrigglesworth,[2] Jennifer Kay,[1] and Steven Vavrus[3]

Received 24 January 2013; revised 22 March 2013; accepted 22 March 2013; published 30 May 2013.

[1] We assess initial-value predictability characteristics of Antarctic sea ice from climate simulations. The integrations are initialized on 1 January with identical ice-ocean-terrestrial conditions and integrated forward for two years. We find that the initialized ice-ocean state provides predictive capability on the ice-edge location around Antarctica for the first several months of integration. During the ice advance season from April to September, significant predictability is retained in some locations with an eastward propagating signal. This is consistent with previous work suggesting the advection of sea ice anomalies with the mean ocean circulation. The ice-edge predictability is then generally lost during the ice retreat season after October. However, predictability reemerges during the next year's ice advance starting around June in some locations. This reemergence is associated with ocean heat content anomalies that are retained at depth during the austral summer and resurface during the following autumn as the ocean mixed layers deepen. **Citation:** Holland, M. M., E. Blanchard-Wrigglesworth, J. Kay, and S. Vavrus (2013), Initial-value predictability of Antarctic sea ice in the Community Climate System Model 3, *Geophys Res Lett.*, *40*, 2121–2124, doi:10.1002/grl.50410.

1. Introduction

[2] Since 1979, a small increase in Antarctic ice extent has occurred with positive Ross Sea trends offset by reductions in the Bellingshausen-Amundsen (B/A) Seas [*Cavalieri and Parkinson*, 2008]. On interannual time scales, the leading mode of Antarctic ice variability exhibits a dipole structure with anomalies of opposite sign in the central/eastern Pacific (about 180°E–240°E) and Atlantic sectors [about 300°E–360°E; *Yuan and Martinson*, 2001]. These anomalies tend to propagate eastward with the ocean circulation [e.g., *White and Peterson*, 1996].

[3] Although mechanisms driving Antarctic sea ice variability have been explored [e.g., *Stammerjohn et al.*, 2008; *Holland and Kwok*, 2012], limited work has investigated the predictability of Antarctic ice. *Chen and Yuan* [2004] developed a statistical model, which produced skillful forecasts for up to a year in advance, particularly in austral winter. *Yuan and Martinson* [2001] used a regression model to show the Antarctic Dipole was predictable with a few month lead. Here we assess Antarctic sea ice predictability characteristics and associated mechanisms using climate simulations. This is similar to studies on Arctic sea ice predictability [e.g., *Blanchard-Wrigglesworth et al.*, 2011, hereafter BW2011; *Chevallier and Salas-Melia*, 2012].

2. Model Experiments

[4] We analyze Community Climate System Model 3 simulations (CCSM3) [*Collins et al.*, 2006]. These are coupled atmosphere-ocean-land-sea ice runs with a resolution of ~1° in the ocean and ice and ~1.4° in the atmosphere. Dynamical ice sheets are not included in CCSM3. Aspects of CCSM3 runs are discussed in a Journal of Climate special issue (Vol. 19, No. 11). While the CCSM3 Antarctic ice is too extensive, the variability is well simulated compared to observations [*Holland and Raphael*, 2006].

[5] A "perfect model" approach is used in which 20 ensemble integrations of the fully coupled CCSM3 are initialized from a CCSM3 run (the "reference run") of the 20th century [*Meehl et al.*, 2006]. For each member, the ice, ocean, and land are initialized with identical 1970 conditions, representative of the late 20th century simulated climate. The atmosphere initial state varies across ensemble runs and is from different years of the 20th century reference run. Given fast time scales of atmospheric variations, this is a reasonable strategy to investigate ice predictability. Initialization data are available once a year on 1 January so ensemble runs are initialized on that date and integrated for two years. This experimental design allows us to assess predictability that arises from knowledge of the initial climate state ("initial value predictability", e.g., BW2011). It gives an upper bound on predictability that can be realized given the assumption of perfect initial conditions and a compatible model. These runs are described fully in *Holland et al.* [2011].

3. Results

[6] To assess initial value predictability, we analyze how the ensemble members diverge over time. When the spread is indistinguishable from simulated natural variability, predictive capability from the initial state is lost. To formalize this, we use the potential prognostic predictability (PPP) [*Pohlmann et al.*, 2004]

$$PPP(t) = 1 - \frac{\sigma_e^2}{\sigma_c^2} \quad (1)$$

where σ_e^2 is the variance across the ensemble members at time t and σ_c^2 is the control climate variance for the relevant month from 300 years of a control run with 1990 greenhouse

[1]National Center for Atmospheric Research, Boulder, Colorado, 80307.
[2]University of Washington, Seattle, Washington, USA.
[3]University of Wisconsin-Madison, Madison, Wisconsin, USA.

Corresponding author: M. M. Holland, National Center for Atmospheric Research, PO Box 3000, Boulder, CO 80307, USA. (mholland@ucar.edu)

©2013. American Geophysical Union. All Rights Reserved.
0094-8276/13/10.1002/grl.50410

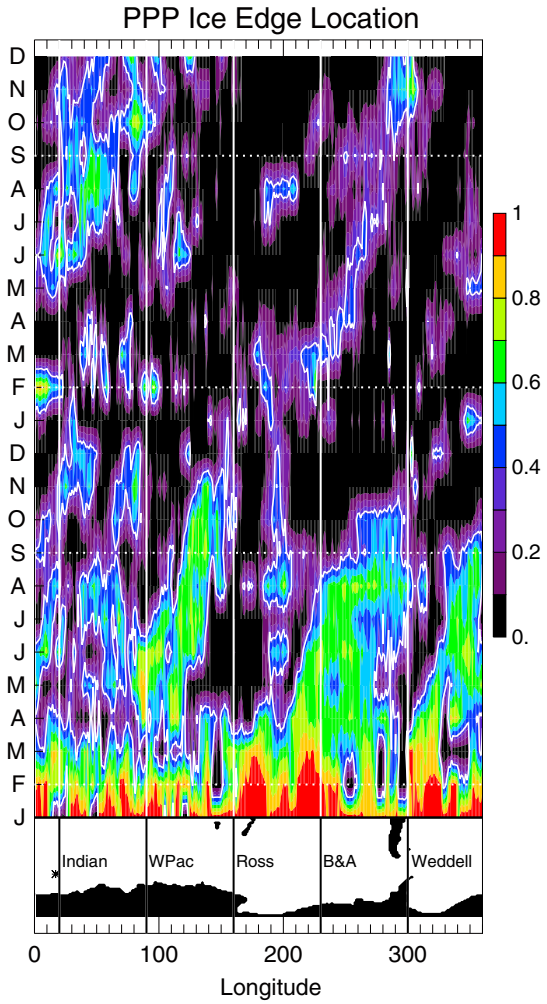

Figure 1. PPP of the ice edge location as a function of longitude and time. The white contour represents values that are significant at the 95% level. The continental outline of Antarctica is shown at the bottom of the plot for reference.

gas levels. PPP of the total ice extent and the ice edge location as a function of longitude are diagnosed. The ice edge location is the northernmost latitude where the southern hemisphere ice concentration exceeds 15%.

3.1. Ice Edge Predictability

[7] Potential prognostic predictability of the ice edge location (Figure 1) indicates that the ice edge is generally predictable for the first three months of integration (JFM). As ice advance begins in April, predictability is lost over areas of the West Pacific and the Ross Sea. Significant predictability is present in the Indian Ocean, but it is scattered in time and space. Significant predictability is consistently present in three regions in April: the western West Pacific, eastern Ross Sea to B/A Sea, and the Weddell Sea. This predictability has an eastward propagating signal over the fall and winter consistent with previous work [*Gloersen and White*, 2001]. As a result, by September predictability is retained in the eastern parts of the three domains.

[8] In the ice retreat season, starting in November, ice extent (Figure 2) and ice edge location (Figure 1) predictability is lost. This occurs as ice retreats into recently ice-covered waters with near-freezing temperatures. The ocean mixed layers shoal

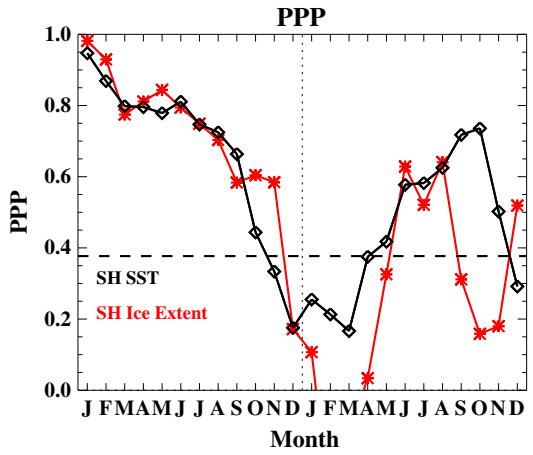

Figure 2. The PPP of sea surface temperature (black) averaged over the high latitude southern ocean (south of 60°S) and total southern hemisphere sea ice extent (red) for the two years of integration. The horizontal dashed line indicates the 95% significance level.

during this time as freshening stabilizes the water column. This leads to little oceanic source of memory for the ice conditions and predictability of the ice edge and total extent is minimal from December to May.

[9] The PPP values (Figures 1, 2) suggest a "reemergence" of predictability during the following years ice advance. In June of year 2, significant predictability is simulated in the eastern Weddell Sea and western Indian Ocean, and is retained in the Indian Ocean through December. There is a hint of reemergence in the B/A Sea starting in April and propagating eastward until December. However, PPP values, while elevated, are only intermittently significant in this region during year two.

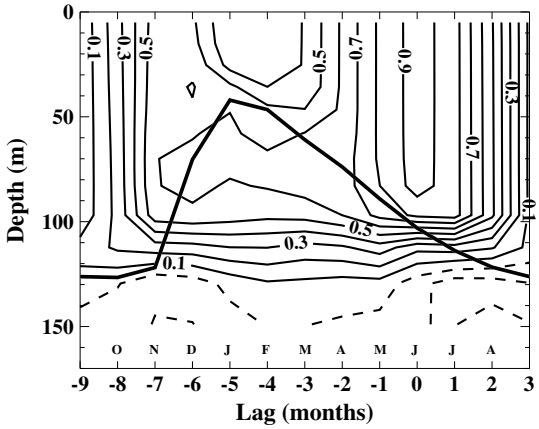

Figure 3. The correlation of sea surface temperature in June at 17°E 62°S with temperatures averaged from 17°E–20°E and 60°S–63°S at different depths and lags (in month) from 100 years of the CCSM3 1990 control integration. The month that corresponds to the individual lag values is shown just above the *x*-axis. The contour interval is 0.1. The zero and negative contours are dashed. The thick black line indicates the climatological maximum mixed layer depth for this region.

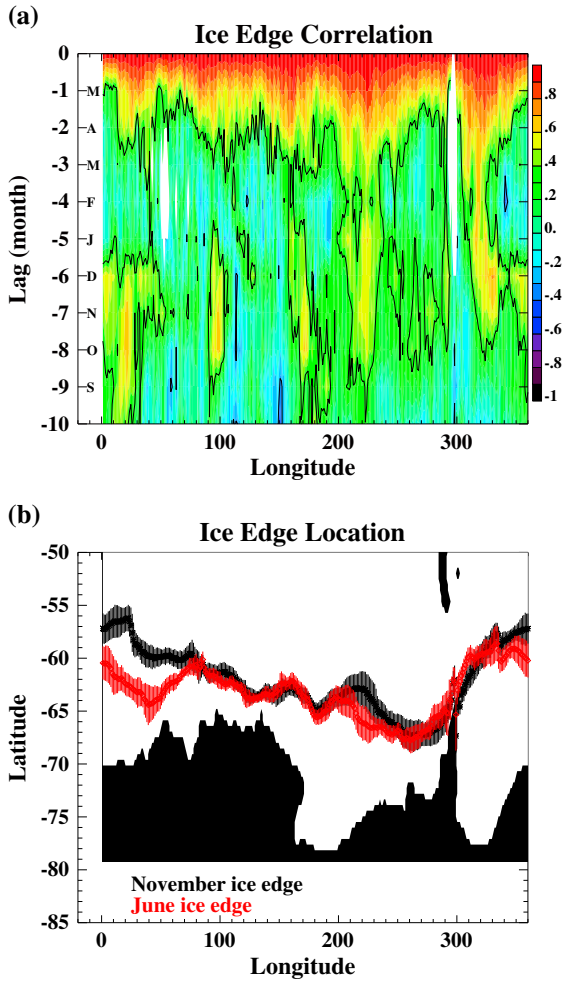

Figure 4. (a) The correlation of the observed June ice edge location with the ice edge location in previous months as a function of longitude. The *y*-axis shows the lag in months. The month that corresponds to the individual lag values is shown just to the right of the *y*-axis. The black contour indicates values that are significant at the 95% level. (b) The observed climatological ice edge location in November and June. The shading of the ice-edge location indicates +/− one standard deviation.

3.2. A Mechanism for Ice Edge Predictability Reemergence

[10] The reemergence of ice edge predictability in the Weddell Sea/Indian Ocean is associated with sea surface temperature anomalies (SSTs) in the region. However, much like the sea ice, the high-latitude SSTs lose predictability over the ice retreat season (Figure 2). This suggests that the source of memory leading to significant predictability in year 2 does not reside in the surface conditions.

[11] From the control integration there is evidence that in some ice-edge locations, November ocean anomalies are retained at depth and reemerge the next June. A similar mechanism has been observed in other regions [e.g., *Alexander et al.*, 1999]. November SST anomalies in the ice-edge region are highly correlated to ice edge variations and shortwave heating. For a location with significant predictability in June of year 2 (Figure 3), the surface heating anomalies extend through the ocean mixed layer. As the mixed layer shoals in summer, the anomalies are isolated from the surface and retained at depth. When the mixed layer deepens the next fall, the heat anomalies resurface, leading to a significant correlation of June SSTs with the prior November conditions, and influencing the ice advance. By this mechanism, variations in the November ice edge can influence the following June sea ice.

[12] The effectiveness of this reemergence mechanism is spatially variable with limited regions of significant predictability in the second year of simulation. As noted, surface advection causes eastward propagation of ice predictability. While velocities are smaller at depth, advection of ocean heat anomalies (sometimes to ice-free regions) can obscure the reemergence signal. It is notable that the region used in the Figure 3 analysis has low speeds at depths where heat anomalies are retained. Other factors influence the effectiveness of the simulated reemergence mechanism. Processes like vertical mixing, can modify ocean temperatures and lead to a loss of correlation. The relative importance of atmospheric forcing for sea ice is spatially variable [e.g., *Stammerjohn et al.*, 2008], influencing ice predictability. Aspects of the mean ice and ocean state may also be important. For example, it appears that sufficiently deep mixed layers are needed for the anomalies to be retained at depth.

3.3. Comparison to Observations

[13] An analysis of the ice edge location from satellite data [*Comiso*, 2000, updated] lends support for a similar reemergence mechanism in observations. In particular, June ice advance anomalies are significantly related to anomalies in the previous November with minimal correlations in most locations in the intervening months (Figure 4) [*Stammerjohn et al.*, 2008]. The location of ice edge anomalies in June and November are similar (Figure 4b). This suggests a mechanism by which anomalous November ice retreat can modify shortwave ocean heating, which then influences ice advance the next June. Presumably November ocean heat anomalies can in part be retained at depth during the ice retreat season and resurface as mixed layers deepen in the fall, similar to the climate modeling results. Given limited gridded ocean observations at depth we cannot confirm this part of the mechanism. However, given the annual cycle of mixed layer depth and the existence of SST reemergence in other locations [*Alexander et al.*, 1999], it appears plausible that this could influence and provide a source of memory for Antarctic sea ice conditions.

4. Conclusions

[14] Initial-value predictability in Antarctic sea ice has been assessed in a perfect model framework. This provides an upper limit on the predictability that could be realized. Our results suggest that with perfect knowledge of conditions on 1 January, the ice edge location is predictable around Antarctica for three months. As ice advances northward starting in April, the ice edge remains predictable in areas of the Western Pacific, the Ross Sea to the B/A Seas, and the Weddell Sea. This exhibits eastward propagation consistent with an advection of anomalies. Predictability is lost as ice retreats toward the continent (from December to May) but reemerges in some areas during ice advance in the second year of simulation. This reemergence is associated with ocean heat anomalies that are

retained at depth over summer and return to the surface as mixed layers deepen during the austral autumn.

[15] These findings, specific to our runs, could be affected by the 1 January initialization date. BW2011 showed that initialization date had little impact on Arctic ice predictability characteristics in similar experiments to those discussed here. An initial evaluation from those experiments (not shown) suggests little influence of the initialization date on Antarctic sea ice predictability. However, more work is needed to diagnose the influence of start-date on initial value predictability.

[16] Some of our Antarctic ice predictability findings resemble those for the Arctic. In particular, the reemergence mechanism in the Southern Ocean also operates in boreal polar regions, where ice anomalies during the growth season are affected by SST anomalies from the previous melt season (BW2011). In addition, time scales of sea ice extent persistence (a few months) are similar in both hemispheres. In the Arctic, summer ice predictability is associated with thickness anomalies (BW2011). This mechanism does not appear to play an important role in the Antarctic where our results suggest little summer ice predictability on multiyear time scales.

[17] **Acknowledgment**. The National Center for Atmospheric Research is sponsored by the National Science Foundation.

[18] The Editor thanks Matthieu Chevallier and an anonymous reviewers for their assistance in evaluating this paper.

References

Alexander, M. A., C. Deser, and M. S. Timlin (1999), The reemergence of SST anomalies in the North Pacific Ocean, *J. Climate*, *12*, 2419–2433.

Blanchard-Wrigglesworth, E., C. M. Bitz, and M. M. Holland (2011), Influence of initial conditions and climate forcing on predicting Arctic sea ice, *Geophys. Res. Lett.*, *38*, L18503, doi:10.1029/2011GL048807.

Chen, D., and X. Yuan (2004), A Markov model for seasonal forecast of Antarctic sea ice, *J. Climate*, *17*, 3156–3168, doi:10.1175/1520-0442(2004)017<3156:AMMFSF>2.0.CO;2.

Chevallier, M., and D. Salas-Melia (2012), The role of sea ice thickness distribution in the Arctic sea ice potential predictability: A diagnostic approach with a couple GCM, *J. Climate*, *25*, 3025–3038, doi:10.1175/JLI-D-11-00209.1.

Collins, W. D., et al. (2006), The Community Climate System Model: CCSM3, *J. Clim.*, *19*(11), 2122–2143, doi:10.1175/JCLI3761.1.

Comiso, J. (2000, updated 2012), Bootstrap Sea Ice Concentrations from Nimbus-7 SMMR and DMSP SSM/I-SSMIS. Version 2, Boulder, Colorado USA: National Snow and Ice Data Center.

Cavalieri, D. J., and C. L. Parkinson, (2008), Antarctic sea ice variability and trends, 1979–2006, *J. Geophys. Res.*, *113*, C07004, doi:10.1029/2007JC004564.

Gloersen, P., and W. B. White (2001), Reestablishing the circumpolar wave in sea ice around Antarctica from one winter to the next, *J. Geophys. Res.*, *106*, 4391–4395.

Holland, M. M., and M. Raphael (2006), Twentieth Century simulation of the Southern Hemisphere in coupled models. Part II: Sea ice conditions and variability, *Clim. Dyn.*, *26*(2–3), 229–246, doi:10.1007/s00382-005-0087-3.

Holland, M. M., D. A. Bailey, and S. Vavrus (2011), Inherent sea ice predictability in the rapidly changing Arctic environment of the Community Climate System Model, version 3, *Clim. Dyn.*, *36*, (7–8), 1239–1253, doi:10.1007/s00382-010-0792-4.

Holland, P. R., and R. Kwok (2012), Wind-driven trends in Antarctic sea-ice drift, *Nat. Geo.*, *5*, 872–875, doi:10.1038/NGEO1627.

Meehl, G. A., et al. (2006), Climate change projections for the Twenty-First century and climate change commitment in the CCSM3, *J. Climate*, *19*(11), 2597–2616, doi:10.1175/JCLI3746.1.

Pohlmann, H., M. Botzet, M. Latif, A. Roesch, M. Wild, and P. Tschuck (2004), Estimating the decadal predictability of a coupled AOGCM, *J. Climate*, *17*(22), 4463–4472, doi:10.1175/3209.1.

Stammerjohn, S. E., D. G. Martinson, R. C. Smith, X. Yuan, and D. Rind (2008), Trends in Antarctic annual sea ice retreat and advance and their relation to El Nino-Southern Oscillation and Southern Annular Model variability, *J. Geophys. Res.*, *113*, C03S90, doi:10.1029/2007JC004269.

White, W. B., and R. G. Peterson (1996), An Antarctic circumpolar wave in surface pressure, wind, temperature and sea ice extent, *Nature*, *380*, 699–702.

Yuan, X., and D. G. Martinson (2001), The Antarctic Dipole and its predictability, *Geophys. Res. Lett.*, *28*, 3609–3612.